

Development of a Platform for Near-Infrared Photoredox Catalysis

Benjamin D. Ravetz, Nicholas E. S. Tay, Candice L. Joe,* Melda Sezen-Edmonds, Michael A. Schmidt, Yichen Tan, Jacob M. Janey, Martin D. Eastgate, and Tomislav Rovis*



Cite This: *ACS Cent. Sci.* 2020, 6, 2053–2059



Read Online

ACCESS |



Metrics & More

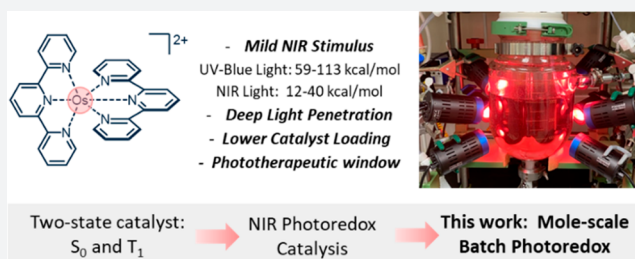


Article Recommendations



Supporting Information

ABSTRACT: Over the past decade, chemists have embraced visible-light photoredox catalysis due to its remarkable ability to activate small molecules. Broadly, these methods employ metal complexes or organic dyes to convert visible light into chemical energy. Unfortunately, the excitation of widely utilized Ru and Ir chromophores is energetically wasteful as ~25% of light energy is lost thermally before being quenched productively. Hence, photoredox methodologies require high-energy, intense light to accommodate said catalytic inefficiency. Herein, we report photocatalysts which cleanly convert near-infrared (NIR) and deep red (DR) light into chemical energy with minimal energetic waste. We leverage the strong spin–orbit coupling (SOC) of Os(II) photosensitizers to directly access the excited triplet state (T_1) with NIR or DR irradiation from the ground state singlet (S_0). Through strategic catalyst design, we access a wide range of photoredox, photopolymerization, and metallaphotoredox reactions which usually require 15–50% higher excitation energy. Finally, we demonstrate superior light penetration and scalability of NIR photoredox catalysis through a mole-scale arene trifluoromethylation in a batch reactor.



INTRODUCTION

The renaissance of synthetic photochemistry in recent years has emerged from major advances in our understanding of the photophysical principles that dictate the interplay between light and matter. While traditional photochemistry relies on the photoexcitation of stoichiometric reagents to overcome challenging thermodynamic barriers, modern photoredox catalysis uses a photon-absorbing molecule—a photocatalyst—to create electronically excited states capable of redox or energy transfer reactions.^{1,2} While synthetic photoredox continues to revolutionize organic chemistry and beyond, key weaknesses remain, including reaction scalability, functional group selectivity, and catalyst robustness.³

One major advance toward improving the scalability of photocatalytic reactions is flow chemistry, in which parallel microreactors overcome the limitations of photon attenuation as described by the Bouguer–Lambert–Beer (BLB) law.⁴ While this strategy is a viable solution from an engineering perspective, it does not address the fundamental inefficiencies inherent to the photocatalysts' photophysical processes.⁵ There are two major issues—first, light penetration into reaction medium is limited by large extinction coefficients (ϵ) associated with the photoexcitation of the photocatalyst's ground state to excited singlet state ($S_0 \rightarrow S_1$ transition) via metal-to-ligand charge transfer (MLCT). For reference, the ϵ of $[\text{Ru}(\text{bpy})_3]^{2+}$ is very large at $\sim 14\,400\text{ M}^{-1}\text{ cm}^{-1}$ (450 nm). Second, accessing the catalytically relevant MLCT triplet state (T_1) requires spin-forbidden intersystem crossing (ISC) from excited singlet to excited triplet state (S_1 to T_1), which is

mediated by spin–orbit coupling (SOC) (Figure 1a). While rapid and efficient ISC is present for many Ru(II) and Ir(III) photocatalysts, it remains a wasteful nonadiabatic process for photoredox with ~ 15 – 25 kcal/mol lost thermally to solvent.⁶

We hypothesize that we could bypass these fundamental issues by leveraging a spin-forbidden $S_0 \rightarrow T_1$ excitation (Figure 1b). $S_0 \rightarrow T_1$ excitation has been reported for Ru(II),⁷ Ir(III),⁸ and Fe(II),⁹ but with inconsequential extinction coefficients for photoredox catalysis. While this concept has been applied to excitation of reagents,^{10,11} identifying new photocatalysts with strong SOC will allow direct access to long-lived redox-active T_1 states via $S_0 \rightarrow T_1$ excitation and minimize ISC-specific energy loss. Fundamentally, this creates a two-state system paradigm for transition metal-based photoredox catalysis by direct $S_0 \rightarrow T_1$ excitation, obviating the limitations associated with accessing the T_1 state by initial $S_0 \rightarrow S_1$ excitation.⁶

Os(II) polypyridyl complexes (Figure 1b) display significant $S_0 \rightarrow T_1$ excitation in the DR and NIR regions (660–800 nm)¹² which is typically attributed to strong SOC induced by Os. When compared to Ru(II) tris-bipyridyl species, Os(II) analogues have relatively shorter excited state lifetimes ($\tau =$

Received: July 17, 2020

Published: October 20, 2020



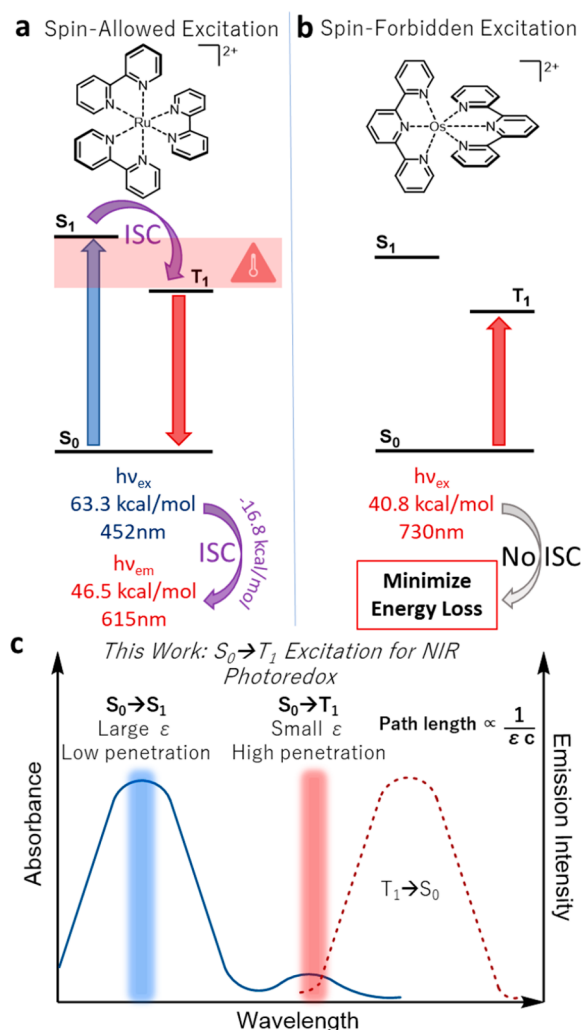


Figure 1. (a) Jablonski schematic for $[\text{Ru}(\text{bpy})_3]^{2+}$. (b) Schematic depicting a $S_0 \rightarrow T_1$ excitation. (c) Comparison of blue and NIR light penetration.

600 ns for $\text{Ru}(\text{bpy})_3^{2+}$ vs 19 ns for $\text{Os}(\text{bpy})_3^{2+}$ in water¹³) due to SOC effects¹⁴ and energy gap considerations.¹⁵ However, Os-based bis-terpyridines have dramatically improved emission lifetimes relative to their Ru congeners ($\tau = 250$ ps for

$\text{Ru}(\text{tpy})_2^{2+}$ vs 269 ns for $\text{Os}(\text{tpy})_2^{2+}$ in MeCN ¹⁶) due to a large energy gap between the $^3\text{MLCT}$ and deactivating ^3MC (metal centered triplet) states.¹⁷ While the luminescence quantum yield for $\text{Os}(\text{tpy})_2^{2+}$ is slightly lower than for $\text{Ru}(\text{bpy})_3^{2+}$,¹⁸ these complexes have been used as triplet sensitizers for singlet oxygen generation¹⁹ and for photon upconversion.²⁰ Their use as photoredox catalysts has yet to be examined and would be interesting due to their red-centered maximum absorption, which enables high solution penetration, as dictated by the BLB law ($\epsilon \sim 500 \text{ M}^{-1} \text{ cm}^{-1}$ (740 nm), which is $\sim 30\times$ lower than $[\text{Ru}(\text{bpy})_3]^{2+}$ at 450 nm). Thus, we envisioned that Os(II) chromophores could catalyze photoredox reactions with improved light penetration (Figure 1c) and a broader material penetration profile^{21,22}—a particularly attractive tool for the emerging fields of photopolymerization²³ and photoenzymatic catalysis.²⁴ For instance, NIR light will penetrate up to 200% further than blue light through most tissues with minimal phototoxicity, which lends itself well to materials applications.²²

RESULTS AND DISCUSSION

We began our studies using $\text{Os}(\text{btpy})_2(\text{PF}_6)_2$ (**Os3**) as the photocatalyst (Figure 2) and performed reactions under NIR light irradiation (Figure 3a). While there are several examples of NIR photoredox catalysis or NIR-initiated photopolymerization^{25–28} using high-powered LEDs, the bulk of photoredox catalysis requires blue or near-UV light. Notably, a recent paper from Gianetti²⁹ describes a helical carbenium photocatalyst for red light driven photoredox catalysis (640 nm).

To elucidate the disparity of visible vs NIR light driven reactions, we draw comparisons to $\text{Ru}(\text{bpy})_3(\text{PF}_6)_2$ which absorbs blue light (63.3 kcal/mol) with high efficiency. However, during ISC it loses 16.8 kcal/mol providing T_1 energy of 46.5 kcal/mol, which is similar to the T_1 energy of **Os3** (40.8 kcal/mol) (Figure 1a,b). From a purely energetic standpoint, this rationalizes the wide oxidizing and reducing capabilities of our NIR photoredox platform despite longer-wavelength light stimulus.

We were excited to achieve a variety of photopolymerizations, ranging from cationic polymerization of cyclohexene oxide (CHO) **2**,³⁰ atom transfer radical polymerization of **5** (ATRP),³¹ or reversible addition–fragmentation chain transfer polymerization (RAFT) of methyl methacrylate (MMA) **8**²⁷

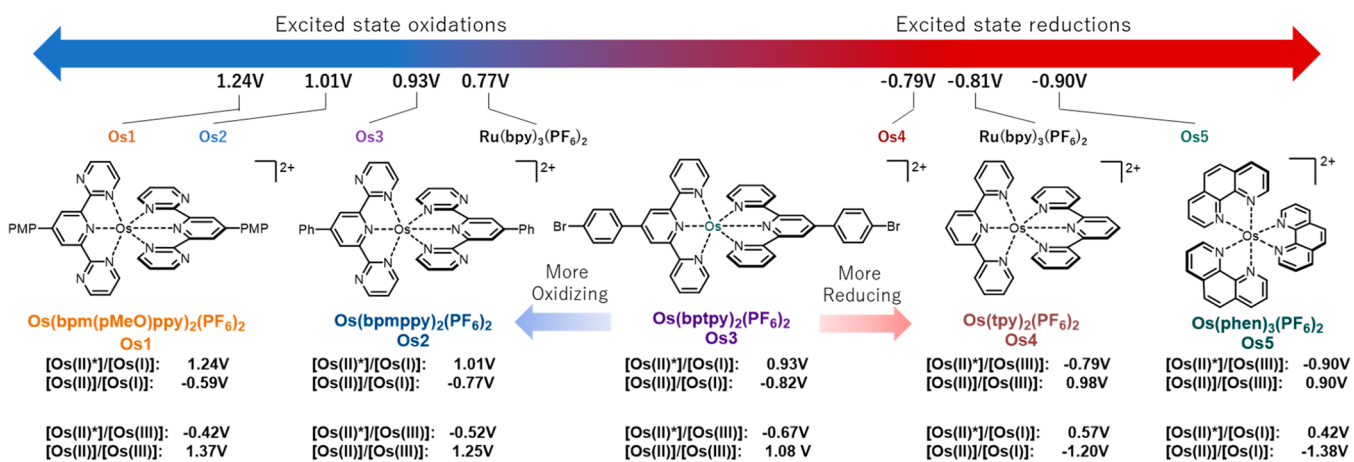


Figure 2. Selected scope of photocatalysts with $S_0 \rightarrow T_1$ transition and their respective redox potentials vs Ag/AgCl in MeCN . Note: The $\text{Os}(\text{II})^*/\text{Os}(\text{I})$ redox couple represents a ligand-centered reduction.

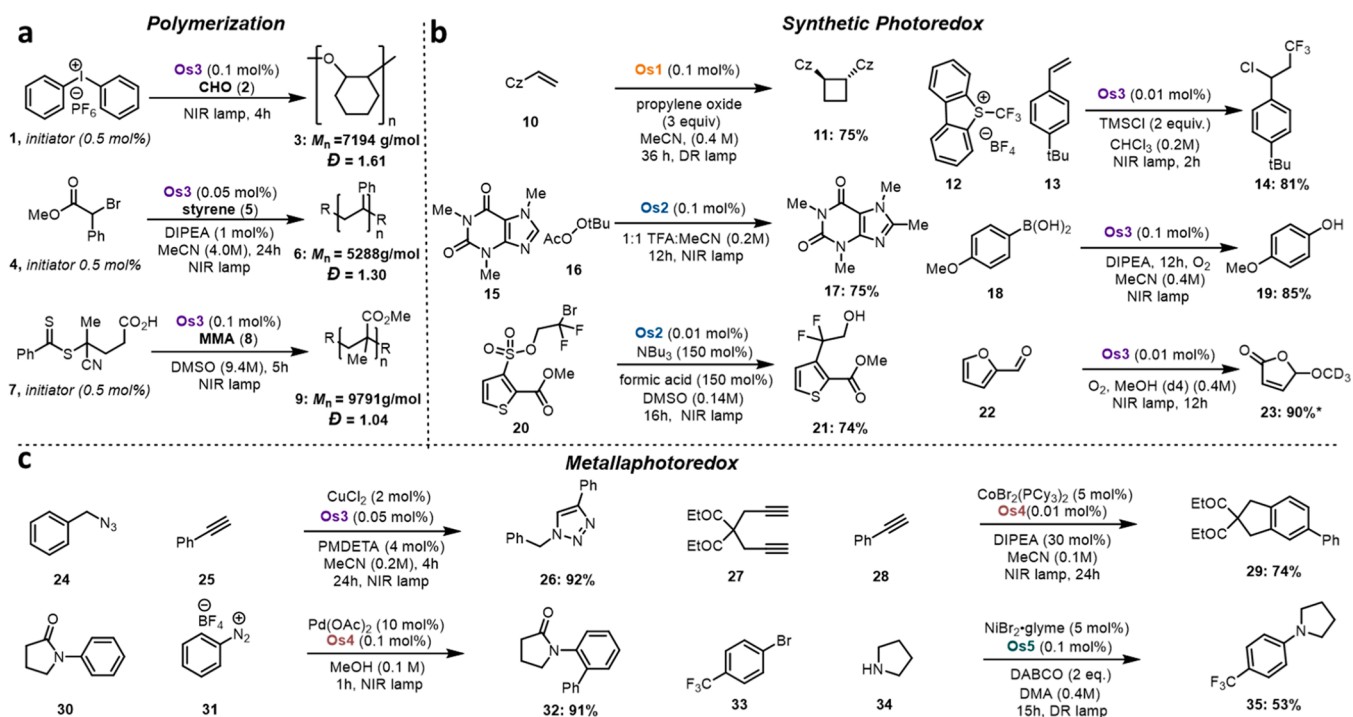


Figure 3. (a) Polymerizations achieved with NIR light. (b) Scope of oxidative and reductive photoredox reactions (yields with * determined by ^1H NMR). (c) Scope of metallaphotoredox reactions including Cu, Co, Ni, and Pd. See Figure S7 for a comparison to original published conditions.

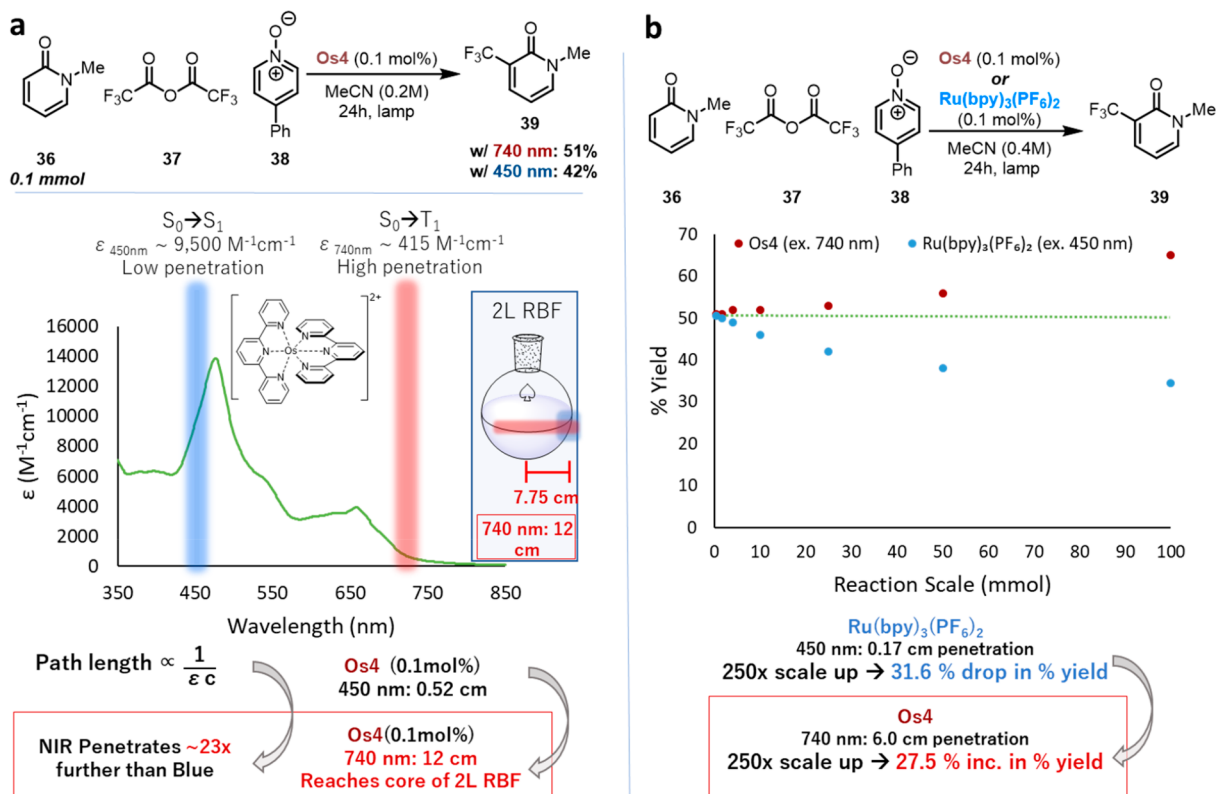


Figure 4. (a) Light penetration comparison of 450 and 740 nm light into reaction mixture. (b) Comparison of 450 nm with Ru(bpy)₃(PF₆)₂ and 740 nm light with Os4 at increasing reaction scale.

(Figure 3a). We next explored transformations that proved challenging with our recently reported method employing triplet fusion upconversion for NIR photoredox catalysis.³² We found that NIR-irradiated Os3 is capable of catalyzing alkene

chlorotrifluoromethylation³³ of 13 in 81% yield. To test the catalyst's stability (Figure S2) under oxidative conditions, we also performed aryl boronic acid oxidation³⁴ and oxygen sensitization (Figure 3b).³⁵ A more oxidizing dipyrimidine

scaffold (**Os1**) catalyzes a cation radical $[2 + 2]$ cycloaddition,³⁶ an intramolecular Smiles reaction,³⁷ and radical methylation.³⁸ In particular, the Smiles reaction is known to be radical-initiated by direct blue light irradiation.³⁹ No rearrangement is observed using NIR light in the absence of Os which eliminates the possibility of a light-activated radical initiation pathway.

Next, we directed our attention on achieving NIR-metal-laphotoredox to expand our scope to cross-couplings, C–H functionalization, and cycloadditions. We observed that NIR irradiation of **Os3** induces the Cu-click reaction.²⁸ The lack of azide radical decomposition of **24** to benzyl amine⁴⁰ is promising for chemical biology applications⁴¹ as this undesirable pathway is observed under high-energy light irradiation⁴² (Figure 3c). While we found **Os3** to be a competent photocatalyst for the Cu-click, it inefficiently activates Co(II) and Pd(II) complexes. Thus, we tuned the terpyridine ligand scaffold to obtain the necessary reduction potentials required to activate Co and Pd (Table S1). We find that Os(tpy)₂(PF₆)₂ (**Os4**) is 120 mV more reducing and enables Pd-catalyzed C–H arylation⁴³ and Co-catalyzed $[2 + 2]$ cycloaddition of alkynes⁴⁴ (Figure 3c). Importantly, diazonium **31**, Pd, and Co intermediates are all competent chromophores for blue light absorption;^{45,46} however, using NIR light to selectively activate **Os4** circumvents light-initiated substrate degradation⁴⁷ and enables lowering of catalyst loading (see Figure S7).

Ni-metallaphotoredox is particularly impactful,⁴⁸ yet we determined that **Os1**–**Os4** are unable to accomplish Ni(II)/Ni(I) reduction. To address this, we turned to trislectic Os(II) complexes which possess a S₀ → T₁ excitation in the deep red (DR) region. Os(phen)₃(PF₆)₂ (**Os5**) enables Ni-catalyzed Buchwald–Hartwig cross-coupling of aryl bromides and amines⁴⁹ under DR irradiation. In light of recent work addressing poor batch scale performance of Ru(bpy)₃(PF₆)₂ under blue light conditions, this is a particularly exciting area of potential impact.^{50,51} The reactions described above demonstrate novel Os and NIR photoredox catalysis, which are performed with up to 200× lower catalyst loadings compared to the literature precedent (for comparisons, see Figure S7).

To highlight the utility of this platform, we investigated the application of Os(II) photocatalysts to reactions in batch. We used Stephenson's arene trifluoromethylation as the model reaction as it has been studied in batch and flow^{52,53} with blue light. Photoredox reactions are typically slower and lower yielding on large scale due to limited light penetration as dictated by the BLB law. As the size of reaction vessels increase, the irradiated surface area to volume ratio decreases such that photon exposure is limiting. While plug flow reactors maximize light penetration and improve reaction rates on kilograms/day scale,⁵⁴ their suitability toward commercial manufacturing is still limited.⁵⁵ From an industrial application perspective, the ability to use batch reactors is incredibly advantageous as it does not require specialized equipment and can be easily implemented in any multipurpose facility.

Our Os catalysts have lower extinction coefficients in the NIR and DR (~500 and ~3500 M⁻¹ cm⁻¹, respectively) (Figure 4a) and bypass the energy losses associated with ISC rendering them more suitable for large-scale reactions in batch reactors. For example, using a catalyst concentration of 0.2 mM and the experimentally determined ϵ values at 450 and 740 nm, we estimate that NIR light penetrates approximately 23-fold further into reaction solution than blue light (Figure 4a).⁵⁶

According to the BLB law, NIR light should penetrate 12 cm into reaction solution before 90% of its power is absorbed by the reaction mixture, whereas blue light can only penetrate 0.52 cm (Figure S5).

We performed Stephenson's trifluoromethylation on various reaction scales (Figure 4b) with Ru(bpy)₃(PF₆)₂ excited by 450 nm light and **Os4** excited by 740 nm light. When blue light and Ru(bpy)₃(PF₆)₂ are used, we observe the yield decrease with increasing reaction scale, aligning with Stephenson's results. However, when **Os4** and 740 nm light are used, we observe the yield maintain or increase on larger reaction scale. We also see an increase in the yield with higher catalyst loading of Os on small scale (2 mol % **Os4**, 65% yield on 1 mmol scale), in contrast to recent findings in which high-powered laser driven flow chemistry alongside decreased catalyst loading was used to improve blue light harvesting within a CTSR.⁵⁵ These findings highlight advantages of **Os4**'s NIR S₀ → T₁ excitation which allows deeper light penetration into the medium.

To fully demonstrate the scalability of our NIR photoredox platform, we opted to test this system on a 1 mol scale to showcase this technology in batch-mode. Inherently, the vessel required to accommodate the 1 mol scale has a large cross-sectional area (22.5 cm outer diameter) and remains a significant challenge for blue light excitation. As diagrammed in Figure 5, we aligned the lamps in an X-like formation around the reactor, which was affixed with overhead stirring, an

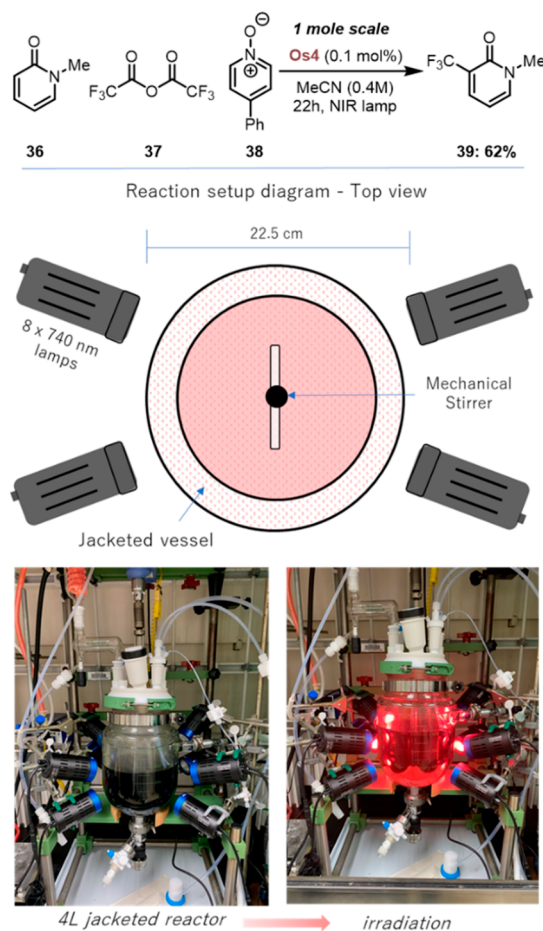


Figure 5. Trifluoromethylation performed on a 1 mol scale in a batch reactor provided 62.6% yield (see the SI).

internal temperature probe, condenser, N₂ sparge line, and sampling line. Upon performing the scale-up with NIR light, we obtained a 62% yield after 22 h of irradiation with eight 740 nm lamps. The reaction stream is dark in color and is conducted at a high concentration (0.4 M). Surprisingly, the yield surpasses the yield obtained on the 10 mmol scale (~50%) after just 6 h of irradiation.

We find the successful scale-up result fascinating since the photon flux on large scale is dramatically decreased compared to the 10 mmol scale. As previously reported and described,⁵² scaling light irradiance proportionally to reaction volume in a batch reactor is a tremendous challenge. For example, to theoretically maintain the same photon flux on a 1 mol scale from a 10 mmol scale, we would require 200 lamps spaced around the reactor (see Figure S8). However, with just 8 lamps, we observe comparable or increased yields.⁵⁷ Taken together, this result demonstrates an excellent proof of concept for scalable photoredox catalysis amenable to batch reactors.

By targeting the NIR S₀ → T₁ excitation, we demonstrate the photophysical advantages of a two-state photoredox system where direct activation of T₁ from S₀ is made possible by SOC. This is broadly applicable across a variety of oxidative and reductive synthesis, photopolymerization, and metallaphotoredox. Ongoing studies aim to redesign photocatalysts to boost the S₀ → T₁ transition, which should improve energy efficiency of catalyst excitation, scalability, and excitation selectivity. We believe these findings will lead to the discovery of new reactions and applications of DR/NIR photoredox catalysis.

■ ASSOCIATED CONTENT

Supporting Information

The Supporting Information is available free of charge at <https://pubs.acs.org/doi/10.1021/acscentsci.0c00948>.

Experimental procedures, characterization data, and copies of ¹H, ¹³C, and ¹⁹F NMR spectra for all new compounds (PDF)

Crystallographic data for Os3 (CIF)

■ AUTHOR INFORMATION

Corresponding Authors

Candice L. Joe – Chemical Process Development, Bristol Myers Squibb, New Brunswick, New Jersey 08903, United States; orcid.org/0000-0002-7167-2416; Email: Candice.joe@bms.com

Tomislav Rovis – Department of Chemistry, Columbia University, New York, New York 10027, United States; orcid.org/0000-0001-6287-8669; Email: tr2504@columbia.edu

Authors

Benjamin D. Ravetz – Department of Chemistry, Columbia University, New York, New York 10027, United States

Nicholas E. S. Tay – Department of Chemistry, Columbia University, New York, New York 10027, United States

Melda Sezen-Edmonds – Chemical Process Development, Bristol Myers Squibb, New Brunswick, New Jersey 08903, United States; orcid.org/0000-0003-0476-6815

Michael A. Schmidt – Chemical Process Development, Bristol Myers Squibb, New Brunswick, New Jersey 08903, United States; orcid.org/0000-0002-4880-2083

Yichen Tan – Chemical Process Development, Bristol Myers Squibb, New Brunswick, New Jersey 08903, United States

Jacob M. Janey – Chemical Process Development, Bristol Myers Squibb, New Brunswick, New Jersey 08903, United States; orcid.org/0000-0001-7697-1709

Martin D. Eastgate – Chemical Process Development, Bristol Myers Squibb, New Brunswick, New Jersey 08903, United States; orcid.org/0000-0002-6487-3121

Complete contact information is available at: <https://pubs.acs.org/doi/10.1021/acscentsci.0c00948>

Notes

The authors declare no competing financial interest.

■ ACKNOWLEDGMENTS

We thank NIGMS (GM125206) and Bristol Myers Squibb for partial support. We thank Eric Simmons (BMS) for helpful discussions. Single crystal X-ray diffraction was performed at the Shared Materials Characterization Laboratory at Columbia University. Use of the SMCL was made possible by funding from Columbia University.

■ REFERENCES

- (1) Romero, N. A.; Nicewicz, D. A. Organic photoredox catalysis. *Chem. Rev.* **2016**, *116*, 10075–10166.
- (2) Prier, C. K.; Rankic, D. A.; MacMillan, D. W. C. Visible light photoredox catalysis with transition metal complexes: applications in organic synthesis. *Chem. Rev.* **2013**, *113*, 5322–5363.
- (3) Tucker, J. W.; Zhang, Y.; Jamison, T. F.; Stephenson, C. R. J. Visible-light photoredox catalysis in flow. *Angew. Chem., Int. Ed.* **2012**, *51*, 4144–4147.
- (4) Cambié, D.; Bottecchia, C.; Straathof, N. J. W.; Hessel, V.; Noël, T. Applications of continuous-flow photochemistry in organic synthesis, material science, and water treatment. *Chem. Rev.* **2016**, *116*, 10276–10341.
- (5) Arias-Rotondo, D. M.; McCusker, J. K. The photophysics of photoredox catalysis: a roadmap for catalyst design. *Chem. Soc. Rev.* **2016**, *45*, 5803–5820.
- (6) Fast ISC from S₁ to T₁ is considered an advantage because the S₁ state has short lifetimes due to spin-allowed electronic or thermal relaxation to S₀ (S₁ → S₀). For example, ISC from the ¹MLCT to the vibrationally excited triplet for Ru(bpy)₃²⁺ occurs in 40 ± 15 fs, with subsequent vibrational cooling to the long-lived triplet state. See: Bhasikuttan, A. C.; Suzuki, M.; Nakashima, S.; Okada, T. Ultrafast fluorescence detection in tris(2,2'-bipyridine)ruthenium(II) complex in solution: relaxation dynamics involving higher excited states. *J. Am. Chem. Soc.* **2002**, *124*, 8398–8405. Thus, accessing the catalytically active triplet via ISC results in a net loss of energy. While photoredox catalysis can also occur through the S₁ state, it is complicated by short excited state lifetimes and competitive back-electron transfer. See ref 1, scheme 5.
- (7) Thompson, D. W.; Ito, A.; Meyer, T. J. [Ru(bpy)₃]^{2+*} and other remarkable metal-to-ligand charge transfer (MLCT) excited states. *Pure Appl. Chem.* **2013**, *85*, 1257–1305.
- (8) Hofbeck, T.; Yersin, H. The triplet state of fac-Ir(ppy)₃. *Inorg. Chem.* **2010**, *49*, 9290–9299.
- (9) Maurer, A. B.; Meyer, G. J. Stark spectroscopic evidence that a spin change accompanies light absorption in transition metal polypyridyl complexes. *J. Am. Chem. Soc.* **2020**, *142*, 6847–6851.
- (10) Kianfar, E.; Apayadin, D. H.; Knör, G. Spin-forbidden excitation: A new approach for triggering photopharmacological processes with low-intensity NIR light. *ChemPhotoChem.* **2017**, *1*, 378–382.
- (11) Nakajima, M.; Nagasawa, S.; Matsumoto, K.; Kuribara, T.; Muranaka, A.; Uchiyama, M.; Nemoto, T. A direct S₀ → T₁ transition in the photoreaction of heavy-atom-containing molecules. *Angew. Chem., Int. Ed.* **2020**, *59*, 6847–6852.

- (12) Imamura, Y.; Kamiya, M.; Nakajima, T. Theoretical study on spin-forbidden transitions of osmium complexes by two-component relativistic time-dependent density functional theory. *Chem. Phys. Lett.* **2016**, *648*, 60–65.
- (13) Creutz, C.; Chou, M.; Netzel, T. L.; Okumura, M.; Sutin, N. Lifetimes, spectra, and quenching of the excited states of polypyridine complexes of Iron(II), ruthenium(II), and osmium(II). *J. Am. Chem. Soc.* **1980**, *102*, 1309–1319.
- (14) Kumaresan, D.; Shankar, K.; Vaidya, S.; Schmehl, R. H. Photochemistry and Photophysics of Coordination Compounds. *Photochemistry and Photophysics of Coordination Compounds I. Top. Curr. Chem.* **2007**, *281*, 101–142.
- (15) Caspar, J. V.; Kober, E. M.; Sullivan, B. P.; Meyer, T. J. Application of the Energy Gap Law to the Decay of Charge-Transfer Excited States. *J. Am. Chem. Soc.* **1982**, *104*, 630–632.
- (16) Sauvage, J. P.; Collin, J. P.; Chambron, J. C.; Guillerez, S.; Coudret, C.; Balzani, V.; Barigelli, F.; De Cola, L.; Flamigni, L. Ruthenium(II) and Osmium(II) Bis(Terpyridine) Complexes in Covalently-Linked Multicomponent Systems: Synthesis, Electrochemical Behavior, Absorption Spectra, and Photochemical and Photophysical Properties. *Chem. Rev.* **1994**, *94*, 993–1019.
- (17) Wächtler, M.; Kübel, J.; Barthelmes, K.; Winter, A.; Schmiedel, A.; Pascher, T.; Lambert, C.; Schubert, U. S.; Dietzek, B. Energy Transfer and Formation of Long-Lived ³MLCT States in Multimetallic Complexes with Extended Highly Conjugated Bis-Terpyridyl Ligands. *Phys. Chem. Chem. Phys.* **2016**, *18*, 2350–2360.
- (18) The luminescence quantum yields for (a) Os(tpy)₂²⁺ and (b) Ru(bpy)₃²⁺ in deaerated MeCN are 0.014 and 0.062, respectively. (a) Benniston, A. C.; Harriman, A.; Li, P.; Sams, C. A. Comparison of the Photophysical Properties of Osmium(II) Bis(2,2':6',2''-Terpyridine) and the Corresponding Ethynylated Derivative. *J. Phys. Chem. A* **2005**, *109* (10), 2302–2309. (b) Caspar, J. V.; Meyer, T. J. Photochemistry of Tris(2,2'-Bipyridine)Ruthenium(2+) Ion (Ru(Bpy)₃²⁺). Solvent Effects. *J. Am. Chem. Soc.* **1983**, *105*, 5583–5590.
- (19) Liu, D.; Zhao, Y.; Wang, Z.; Xu, K.; Zhao, J. Exploiting the benefit of S₀ → T₁ excitation in triplet–triplet annihilation upconversion to attain large anti-stokes shifts: Tuning the triplet state lifetime of a tris(2,2'-bipyridine) osmium(II) complex. *Dalton Trans.* **2018**, *47*, 8619–8628.
- (20) Sasaki, Y.; Amemori, S.; Kouno, H.; Yanai, N.; Kimizuka, N. Near infrared-to-blue photon upconversion by exploiting direct S–T absorption of a molecular sensitizer. *J. Mater. Chem. C* **2017**, *5*, 5063–5067.
- (21) It should be noted that toxicity concerns for Os complexes are entirely predicated on OsO₄, the complex for which the greatest body of Os toxicity has been determined. It is also noteworthy that Os polypyridyl complexes have been used in cellular imaging with no apparent toxicity; see (a) Byrne, A.; et al. Osmium(II) polypyridyl polyarginine conjugate as a probe for live cell imaging; a comparison of uptake, localization and cytotoxicity with its ruthenium(II) analogue. *Dalton Trans.* **2015**, *44*, 14323–14332. (b) Huang, R.; et al. Chiral Os(II) polypyridyl complexes as enantioselective nuclear DNA imaging agents especially suitable for correlative high-resolution light and electron microscopy studies. *ACS Appl. Mater. Interfaces* **2020**, *12*, 3465–3473.
- (22) Szacilowski, K.; Macyk, W.; Drzewiecka-Matuszek, A.; Brindell, M.; Stochel, G. Bioinorganic photochemistry: frontiers and mechanisms. *Chem. Rev.* **2005**, *105*, 2647–2694.
- (23) Chen, M.; Zhong, M.; Johnson, J. A. Light-controlled radical polymerization: mechanisms, methods, and applications. *Chem. Rev.* **2016**, *116*, 10167–10211.
- (24) Schmermund, L.; Jurkaš, V.; Özgen, F. F.; Barone, G. D.; Büchsenhüt, H. C.; Winkler, C. K.; Schmidt, S.; Kourist, R.; Krouitl, W. Photo-biocatalysis: biotransformations in the presence of light. *ACS Catal.* **2019**, *9*, 4115–4144.
- (25) Schmitz, C.; Pang, Y.; Gülz, A.; Gläser, M.; Horst, J.; Jäger, M.; Strehmel, B. New high-power LEDs open photochemistry for near-infrared-sensitized radical and cationic photopolymerization. *Angew. Chem., Int. Ed.* **2019**, *58*, 4400–4404.
- (26) (a) Chen, Z.; Oprych, D.; Xie, C.; Kutahya, C.; Wu, S.; Strehmel, B. Upconversion-nanoparticle-assisted radical polymerization at λ=974 nm and the generation of acidic cations. *ChemPhotoChem.* **2017**, *1*, 499–503. (b) Freitag, M.; Möller, N.; Rühling, A.; Strassert, C. A.; Ravoo, B. J.; Glorius, F. Photocatalysis in the dark: Near infrared light driven photoredox catalysis by an upconversion nanoparticle/photocatalyst system. *ChemPhotoChem.* **2019**, *3*, 24–27.
- (27) Xu, J.; Shanmugam, S.; Duong, H. T.; Boyer, C. Organophotocatalysts for photoinduced electron transfer-reversible addition–fragmentation chain transfer (PET-RAFT) polymerization. *Polym. Chem.* **2015**, *6*, 5615–5624.
- (28) Kutahya, C.; Yagci, Y.; Strehmel, B. Near-infrared photoinduced copper-catalyzed azide-alkyne click chemistry with a cyanide comprising a barbiturate group. *ChemPhotoChem.* **2019**, *3*, 1180–1186.
- (29) Mei, L.; Veleta, J. M.; Gianetti, T. L. Helical carbenium ion: A versatile organic photoredox catalyst for red-light-mediated reactions. *J. Am. Chem. Soc.* **2020**, *142*, 12056–12061.
- (30) Tasdelen, M. A.; Kumbaraci, V.; Jockusch, S.; Turro, N. J.; Talinli, N.; Yagci, Y. Photoacid generation by stepwise two-photon absorption: photoinitiated cationic polymerization of cyclohexene oxide by using benzodioxinone in the presence of iodonium salt. *Macromolecules* **2008**, *41*, 295–297.
- (31) Singh, V. K.; et al. Highly efficient organic photocatalysts discovered via a computer-aided-design strategy for visible light-driven atom transfer radical polymerization. *Nature Catalysis* **2018**, *1*, 794–804.
- (32) Ravetz, B. D.; Pun, A. B.; Churchill, E. M.; Congreve, D. N.; Rovis, T.; Campos, L. M. Photoredox catalysis using infrared light via triplet fusion upconversion. *Nature* **2019**, *565*, 343–346.
- (33) Carboni, A.; Dagousset, G.; Magnier, E.; Masson, G. Three-component photoredox-mediated chloro-, bromo-, or iodotrifluoromethylation of alkenes. *Synthesis* **2015**, *47*, 2439–2445.
- (34) Zou, Y.-Q.; Chen, J.-R.; Liu, X.-P.; Lu, L.-Q.; Davis, R. L.; Jørgensen, K. A.; Xiao, W.-J. Highly efficient aerobic oxidative hydroxylation of arylboronic acids: photoredox catalysis using visible light. *Angew. Chem.* **2012**, *124*, 808–812.
- (35) Meyers, A. I.; Nolen, R. L.; Collington, E. W.; Narwid, T. A.; Strickland, R. C. Total synthesis of camptothecin and desethyl-desoxycamptothecin. *J. Org. Chem.* **1973**, *38*, 1974–1983.
- (36) Riene, M.; Nicewicz, D. A. Synthesis of cyclobutanelignans via an organic single electron oxidant–electron relay system. *Chem. Sci.* **2013**, *4*, 2625–2629.
- (37) Douglas, J. J.; Albright, H.; Sevrin, M. J.; Cole, K. P.; Stephenson, C. R. J. A visible light-mediated radical smiles rearrangement and its application to the synthesis of a difluorospiracyclic ORL-1 antagonist. *Angew. Chem., Int. Ed.* **2015**, *54*, 14898–14902.
- (38) DiRocco, D. A.; Dykstra, K.; Krska, S.; Vachal, P.; Conway, D. V.; Tudge, M. Late-stage functionalization of biologically active heterocycles through photoredox catalysis. *Angew. Chem., Int. Ed.* **2014**, *53*, 4802–4806.
- (39) Douglas, J. J.; Sevrin, M. J.; Cole, K. P.; Stephenson, C. R. J. Preparative scale demonstration and mechanistic investigation of a visible light-mediated radical smiles rearrangement. *Org. Process Res. Dev.* **2016**, *20*, 1148–1155.
- (40) Chen, Y.; Kamlet, A. S.; Steinman, J. B.; Liu, D. R. A biomolecule-compatible visible-light-induced azide reduction from a DNA-encoded reaction-discovery system. *Nat. Chem.* **2011**, *3*, 146–153.
- (41) Soriano del Amo, D.; Wang, W.; Jiang, H.; Besanceney, C.; Yan, A. C.; Levy, M.; Liu, Y.; Marlow, F. L.; Wu, P. Biocompatible copper(I) catalysts for in vivo imaging of glycans. *J. Am. Chem. Soc.* **2010**, *132*, 16893–16899.
- (42) Angerani, S.; Winssinger, N. Visible light photoredox catalysis using ruthenium complexes in chemical biology. *Chem. - Eur. J.* **2019**, *25*, 6661–6672.

(43) Kalyani, D.; McMurtrey, K. B.; Neufeldt, S. R.; Sanford, M. S. Room-temperature C–H arylation: merger of Pd-catalyzed C–H functionalization and visible-light photocatalysis. *J. Am. Chem. Soc.* **2011**, *133*, 18566–18569.

(44) Ruhl, K. E.; Rovis, T. Visible light-gated cobalt catalysis for a spatially and temporally resolved [2+2+2] cycloaddition. *J. Am. Chem. Soc.* **2016**, *138*, 15527–15530.

(45) Chuentragool, P.; Kurandina, D.; Gevorgyan, V. Catalysis with palladium complexes photoexcited by visible light. *Angew. Chem., Int. Ed.* **2019**, *58*, 11586–11598.

(46) Ravetz, B. D.; Wang, J. Y.; Ruhl, K. E.; Rovis, T. Photoinduced ligand-to-metal charge transfer enables photocatalyst-independent light-gated activation of Co(II). *ACS Catal.* **2019**, *9*, 200–204.

(47) Mahouche-Chergui, S.; Gam-Derouich, S.; Mangeney, C.; Chehimi, M. M. Aryl diazonium salts: a new class of coupling agents for bonding polymers, biomacromolecules and nanoparticles to surfaces. *Chem. Soc. Rev.* **2011**, *40*, 4143–4166.

(48) Twilton, J.; Le, C.; Zhang, P.; Shaw, M. H.; Evans, R. W.; MacMillan, D. W. C. The merger of transition metal and photocatalysis. *Nat. Rev. Chem.* **2017**, *1*, 0052.

(49) Corcoran, E. B.; Pirnot, M. T.; Lin, S.; Dreher, S. D.; DiRocco, D. A.; Davies, I. W.; Buchwald, S. L.; MacMillan, D. W. C. Aryl amination using ligand-free Ni(II) salts and photoredox catalysis. *Science* **2016**, *353*, 279–283.

(50) Park, B. Y.; Pirnot, M. T.; Buchwald, S. L. Visible light-mediated (hetero)aryl amination using Ni(II) salts and photoredox catalysis in flow: a synthesis of Tetracaine. *J. Org. Chem.* **2020**, *85*, 3234–3244.

(51) Kudisch, M.; Lim, C.-H.; Thordarson, P.; Miyake, G. M. Energy transfer to Ni-amine complexes in dual catalytic, light-driven C–N cross-coupling reactions. *J. Am. Chem. Soc.* **2019**, *141*, 19479–19486.

(52) Beatty, J. W.; Douglas, J. J.; Miller, R.; McAtee, R. C.; Cole, K. P.; Stephenson, C. R. J. Photochemical perfluoroalkylation with pyridine N-oxides: mechanistic insights and performance on a kilogram scale. *Chem.* **2016**, *1*, 456–472.

(53) Beatty, J. W.; Douglas, J. J.; Cole, K. P.; Stephenson, C. R. J. A scalable and operationally simple radical trifluoromethylation. *Nat. Commun.* **2015**, *6*, 7919.

(54) Elliott, L. D.; Berry, M.; Harji, B.; Klauber, D.; Leonard, J.; Booker-Milburn, K. I. A small-footprint, high-capacity flow reactor for UV photochemical synthesis on the kilogram scale. *Org. Process Res. Dev.* **2016**, *20*, 1806–1811.

(55) Harper, K. C.; Moschetta, E. G.; Bordawekar, S. V.; Wittenberger, S. J. A laser driven flow chemistry platform for scaling photochemical reactions with visible light. *ACS Cent. Sci.* **2019**, *5*, 109–115.

(56) Light penetration distance is purely a function of selected excitation wavelength. Os1–5 penetration depths can be tuned by targeting $S_0 \rightarrow S_1$ or $S_0 \rightarrow T_1$, while $[\text{Ru}(\text{bpy})_3]^{2+}$ only has the $S_0 \rightarrow S_1$ available.

(57) A reaction quantum yield determination would clearly be of value. However, a consistent and widely accepted chemical standard for NIR actinometry (740 nm) remains to be developed. For a recent development of a universal actinometer applicable up to 700 nm, and a discussion of the state of the art, see: Reinfelds, M.; Hermanns, V.; Halbritter, T.; Wachtveitl, T.; Braun, M.; Slanina, T.; Heckel, A. A robust, broadly absorbing fulgide derivative as a universal chemical actinometer for the UV to NIR region. *ChemPhotoChem.* **2019**, *3*, 441–449.